







# Interaction time of Schrödinger cat states with a periodically driven quantum system: Symplectic covariance approach

D. Woźniak , B. J. Spisak ,\* M. Kalka , M. Wołoszyn , M. Wleklińska , and P. Pigoń 

*AGH University of Krakow, Faculty of Physics and Applied Computer Science,  
and aleja A. Mickiewicza 30, 30-059 Krakow, Poland*

D. Kołaczek 

*Department of Applied Mathematics, University of Agriculture in Kraków, ulica Balicka 253c, 30-198 Kraków, Poland*



(Received 27 March 2024; accepted 16 July 2024; published 12 August 2024)

The symplectic invariance property of the Wigner-Rényi entropies family is used to estimate the interaction time for the propagating Schrödinger cat state that interacts with the periodically changing potential. With the help of this property, the hierarchy of the interaction times is specified for the quantum dynamics of the periodically driven system. It is also demonstrated that the lower and upper bounds of the interaction time are determined by the Wigner-Rényi entropies corresponding to increasing Rényi index values, respectively. The interpretation of the presented results is supported by calculations of the dynamical transmission and capture coefficients, which give a clear insight into the scattering of the non-Gaussian state on the periodically changing potential, which switches between the Gaussian potential barrier and the well.

DOI: [10.1103/PhysRevA.110.022416](https://doi.org/10.1103/PhysRevA.110.022416)

## I. INTRODUCTION

Physical systems interacting with an explicitly time-dependent periodic external force are referred to as periodically driven systems [1]. In recent times, a notable surge in research efforts dedicated to unraveling the intricate dynamics exhibited by such systems has been witnessed. The widespread applications of the periodic driving include the ratchet effect, both quantum [2,3] and classical [4,5], laser interactions [6], Bose condensation [7], and, even further, such systems are employed in the studies of topological insulators [8,9], time crystals [10], or periodically driven optical lattices [11]. Various formulations of quantum theory can be utilized to describe the dynamics of periodically driven quantum systems, helping to highlight different features of their behavior [1,12]. Here, we explore the dynamics of periodically driven quantum systems within the phase-space framework in which the state of the system is represented by the Wigner distribution function (WDF). Using this approach, it is possible not only to gain deeper insights into the behavior of the system in the domain of conjugated variables (e.g., momentum and position), but also to acquire correspondence with the classical dynamics [13]. The approach based on the concept of the WDF has found a wide range of applications, from quantum optics [14,15] and quantum information [16–18], through quantum chemistry [19–21] and biology [22,23], to Bose-Einstein condensates [24–27] or quantum Brownian motion [28–30]. It has recently also been applied in the study of periodically driven systems [31]. Notably, the WDF can take negative values in some regions of the phase

space. This property prevents the interpretation of the WDF as a proper probability distribution function on the phase space. Due to this distinctive property, the WDF is also used to detect and study the nonclassicality of quantum states [32]. Another characteristic that distinguishes the WDF and provides additional insight into the considered quantum system is the symplectic covariance [33–37]. Not only does the area occupied by the WDF in the phase space remain unchanged under symplectic transformations (shear, rotation, or scaling), but there are also WDF-dependent functions whose integrals over the phase space remain constant when the time evolution of the WDF is given by symplectic transformations (e.g., motion in the free space). Such integrals can be used to define the so-called symplectically invariant measures, which can be used to detect the state interaction with the potential barrier in the scattering experiments. From many symplectically invariant measures, it is worth distinguishing phase-space entropic measures. They are particularly relevant if one looks at the phase-space formulation of quantum theory as a statistical theory in which entropic quantities play a key role in describing the physical system. Among many formulations of phase-space entropies based on the WDF [38,39] and other phase-space distributions [40], we would like to focus on the Wigner-Rényi entropy [39,41]. This measure, depending on the Rényi parameter, allows the determination of phase-space analogues of well-established entropic measures in statistical theory (e.g., Shannon entropy, collisional entropy, maximum entropy) and, furthermore, for a one-half Rényi index, it can be interpreted as a measure of nonclassicality of the state [41]. As we previously showed, the symplectic covariance of a dynamical measure can be successfully employed to determine the interaction time of a quantum state, with the potential barrier given by the absolutely integrable function.

\*Contact author: [bjs@agh.edu.pl](mailto:bjs@agh.edu.pl)

This approach provides a new perspective on the decades-old and often confusing problem of establishing the barrier crossing time [42]. Over the years, many different theories have been developed, which have given plenty of opportunities to determine how long it takes to pass through the barrier. Therefore, in this work, we would like not only to determine another interaction time, but also to prove that the interaction time obtained from symplectically invariant measures allows us to indicate an upper and lower limit on such interaction time.

In this paper, by employing entropic measures, we show how to apply a symplectic covariance approach to estimating interaction time within a periodically driven system. Including entropic measures when calculating interaction time in a periodically driven system is beneficial as they offer insights into the intricate relationship dynamics, facilitating a deeper comprehension of system behavior and temporal interactions. Owing to that, we were able to bound the interaction time and show that the lowest barrier crossing times can be achieved by using the Wigner-Rényi entropy with one-half Rényi index.

The paper is organized as follows. Section II consists of the theoretical background in a nutshell and a description of the used numerical algorithm. In Sec. III, we present the results and their discussion. Section IV contains a summary and conclusions. Finally, the paper ends with appendices that contain a detailed derivation of the presented algorithm and a proof of the monotonicity property of the Wigner-Rényi entropies for continuous probability distribution functions.

## II. THEORETICAL FRAMEWORK

### A. Phase-space dynamics and symplectic invariance

In the phase-space representation of quanta, any isolated quantum-mechanical system is characterized by the Weyl symbol of the Hamiltonian [43,44]. In particular, this symbol for the one-particle system in one dimension has a form consistent with its classical counterpart, i.e., this is a real function of the position and the momentum defined on the two-dimensional phase space generated by these two canonically conjugated variables and can be written in the form  $H(x, p) = p^2/(2m) + U(x)$ , where  $m$  is the mass,  $p$  is the momentum,  $x$  is the position, and  $U(x)$  is the potential energy. It is important to remember that the momentum and the position occurring in this formula are the Weyl symbols corresponding to these quantities. However, this form of the Hamiltonian is insufficient for the description of time-dependent systems presented in Sec. I. Motivated by this deficiency, we generalize the Hamiltonian mentioned above to the time-dependent form. For this purpose, we assume that the new one-particle Hamiltonian explicitly depends on the time through the potential part, denoted by  $W(x, t)$ . Furthermore, we assume its separable form, namely,  $W(x, t) = U(x)\Sigma(t)$ , where  $U(x)$  is the spatial part, and the function  $\Sigma(t)$  is the temporal part of this term. Taking into account these assumptions, we can characterize the time-dependent system under consideration by the Weyl symbol of the effective Hamiltonian in the form

$$H(x, p, t) = \frac{p^2}{2m} + U(x)\Sigma(t). \quad (1)$$

The specification of the functions  $U(x)$  and  $\Sigma(t)$  is given later in this work.

Within the phase-space representation, the WDF can express the state of this time-dependent system. This real and normalized function can take negative values in some regions of the phase space for some states. In fact, this property disqualifies the intuitive interpretation of the WDF as a proper probability distribution function on the phase space despite having well-defined marginals. On the other hand, this property is often used to indicate the quantumness of the system state represented by the WDF [32]. In the case when the system is in a pure state, the corresponding WDF is given by the formula [45]

$$\varrho(x, p, t) = \frac{1}{2\pi\hbar} \int_{\mathbb{R}} dX \psi^*\left(x + \frac{X}{2}, t\right) \psi\left(x - \frac{X}{2}, t\right) e^{-\frac{i}{\hbar} pX}, \quad (2)$$

where, for each time instant,  $t \in \mathbb{R} : \psi(\cdot, t) \in L^2(\mathbb{R}, dx)$  is the time-dependent Schrödinger wave function and the asterisk symbol denotes the complex conjugate. The time evolution of the WDF is determined by the solution of the Cauchy problem for the Moyal equation,

$$\begin{aligned} \partial_t \varrho(x, p, t) &= -i\hat{\mathcal{L}}_M(t)\varrho(x, p, t), \quad t > 0 \\ \varrho(x, p, 0) &= \varrho_0(x, p), \end{aligned} \quad (3)$$

where  $\varrho_0(x, p)$  represents the initial condition and  $\hat{\mathcal{L}}_M(t)$  is the Moyal operator defined by the formula

$$\begin{aligned} -i\hat{\mathcal{L}}_M(t) &:= -\frac{p}{m}\partial_x + \frac{1}{i\hbar}\Sigma(t)\left[U\left(x + \frac{i\hbar}{2}\partial_p\right) \right. \\ &\quad \left. - U\left(x - \frac{i\hbar}{2}\partial_p\right)\right]. \end{aligned} \quad (4)$$

Alternatively, the expression in the square bracket of the second term in the right-hand side of the Moyal operator (4) can be written in a differential form, namely,

$$\begin{aligned} \hat{\mathcal{L}}_M(t) &= i\left\{-\frac{p}{m}\partial_x + \Sigma(t)[\partial_x U(x)]\partial_p\right\} \\ &\quad + i\sum_{r=1}^{\infty} \frac{(-1)^r \Sigma(t)}{(2r+1)!} \left(\frac{\hbar}{2}\right)^{2r} \partial_x^{2r+1} U(x) \partial_p^{2r+1}. \end{aligned} \quad (5)$$

Owing to this, the physical interpretation of the operator (5) seems to be more transparent. Namely, the first term in the right-hand side of this expression corresponds to the Liouville operator [46]. This operator generates the classical dynamics of the WDF in the phase space, i.e., its center of mass moves along the classical trajectory resulting from the solution of the Hamilton equations. In turn, the second term, i.e., a series called a Moyal expansion, represents the operator related to quantum effects. This term describes the perturbations of the classical dynamics of the WDF by systematically considering increasingly high-order terms in the Moyal expansion. This is why the full quantum dynamics of the WDF emerges from the Moyal equation. Let us note that this approach allows one to look at quantum dynamics as the deformation of the classical one, and the Planck constant measures this deformation. One more thing that results from this approach is worth noting. Namely, the Moyal equation reduces to the mere Liouville equation for polynomial potentials of the order less than or

equal to 2. This result leads to the important conclusion that the classical and quantum dynamics of the WDF are precisely the same for this class of potentials. In this case, the time dependence of the wave function, appearing in Eq. (2) by definition, is determined by the metaplectic time-evolution operator [47], and the corresponding time evolution of the WDF is given by point transformation, represented by the appropriate symplectic matrix  $\mathbf{S}_t$ . This property is known as a symplectic covariance of WDF [34]. Using this property, one might notice that all integrals of the form

$$I(t) = \int_{\mathbb{R}^2} dx dp f[\varrho(x, p, t)], \quad (6)$$

defined for any function  $f : [-1/(\pi\hbar), 1/(\pi\hbar)] \rightarrow \mathbb{R}$  such that the composition  $(x, p) \mapsto (f \circ \varrho)(x, p, t)$  is integrable on  $\mathbb{R}^2$  for every  $t \geq 0$ , are invariant with respect to such transformations, namely,

$$\begin{aligned} I(t) &= \int_{\mathbb{R}^2} dx dp f\{\varrho_0[\mathbf{S}(t)(x, p)^T]\} \\ &= \int_{\mathbb{R}^2} dx dp f[\varrho_0(x, p)] = I(0), \end{aligned} \quad (7)$$

where for point transformations given by symplectic matrices, the Jacobian determinant is equal to 1. For any  $f$  defined by the conditions above, we say that  $I(t)$  is an invariant measure. It is worth mentioning that in the context of the time evolution of the quantum systems, the maximal covariance group of the WDF consists solely of symplectic transformations [36]. From the point of view of this work, two particularly interesting cases of symplectic covariance arise from the evolution of the WDF in potentials of the zeroth and second order. Physically, they correspond to the cases of free-particle and harmonic-oscillator potentials. The Moyal equation for the harmonic oscillator,  $U(x) = m\omega^2 x^2/2$ , where  $\omega$  is the angular frequency, has the form

$$\partial_t \varrho(x, p, t) + \frac{p}{m} \partial_x \varrho(x, p, t) - m\omega x \partial_p \varrho(x, p, t) = 0. \quad (8)$$

For the given initial condition  $\varrho_0(x, p)$ , the solution of Eq. (8) is

$$\begin{aligned} \varrho(x, p, t) &= \varrho_0 \left[ x \cos(\omega t) - \frac{p}{m\omega} \sin(\omega t), p \cos(\omega t) \right. \\ &\quad \left. + x m \omega \sin(\omega t) \right]. \end{aligned} \quad (9)$$

This motion is the elliptical rotation in the phase space and, consequently, we conclude that the values of the WDF are preserved along the classical trajectory. Based on this result, we can also find the solution of the free-space Moyal equation by calculating the limit of Eq. (9) for  $\omega \rightarrow 0$ . The obtained result is the following:

$$\varrho(x, p, t) = \varrho_0 \left( x - \frac{p}{m} t, p \right). \quad (10)$$

In this case, the motion of the WDF is given by the shearing transformation. The meaning of the solutions given by Eq. (9) and Eq. (10) is crucial for our studies, as they both fulfill the previously mentioned invariance condition given by Eq. (6). This expresses the fact that the value of the integral of any function  $f$  composed with rotated or sheared WDF does not

change with respect to the integral of  $f$  composed with the initial condition. This property is crucial for our further studies of the interaction time based on the symplectically invariant measures. Let us now focus on the previously defined Cauchy problem for the Moyal equation given by Eq. (3). Its formal solution can be written in the form

$$\varrho(x, p, t) = \hat{\mathcal{U}}(t, 0) \varrho_0(x, p), \quad (11)$$

where  $\hat{\mathcal{U}}(t, 0) \equiv \hat{\mathcal{U}}(t)$  is the time-evolution operator whose form is given by the time-ordered exponential operator,

$$\hat{\mathcal{U}}(t, 0) = \hat{\mathcal{T}} \exp \left[ -i \int_0^t dt' \hat{\mathcal{L}}_M(t') \right], \quad (12)$$

wherein  $\hat{\mathcal{T}}$  stands for the time ordering [48,49]. Therefore, the WDF at time  $t + \Delta t$ , where  $\Delta t$  is a finite time increment, can be expressed by the formula

$$\varrho(x, p, t + \Delta t) = \hat{\mathcal{T}} \exp \left[ -i \int_t^{t+\Delta t} dt' \hat{\mathcal{L}}_M(t') \right] \varrho_0(x, p, t). \quad (13)$$

On the other hand, using the results of Suzuki [50], any time-ordered exponential operator can be expressed by the ordinary exponential operator in the form

$$\hat{\mathcal{T}} \exp \left[ -i \int_0^t dt' \hat{\mathcal{L}}_M(t') \right] = \exp \{ [\hat{\mathcal{L}}_M(t) + \hat{D}] \Delta t \}, \quad (14)$$

where the operator  $\exp(\hat{D}\Delta t)$ , defined by the formula

$$\hat{F}(t) \exp(\hat{D}\Delta t) \hat{G}(t) = \hat{F}(t + \Delta t) \hat{G}(t), \quad (15)$$

is called the left-time shift operator and formally is expressed by the differential operator, i.e.,  $\hat{D} = \overleftarrow{\partial}_t$ , where the arrow indicates in which direction the derivative acts. Owing to this, combining Eqs. (13) and (14), we obtain the expression for the WDF at the instant time  $t + \Delta t$  in the following form:

$$\varrho(x, p, t + \Delta t) = \exp \{ [\hat{\mathcal{L}}_M(t) + \hat{D}] \Delta t \} \varrho(x, p, t). \quad (16)$$

The expression obtained in this way has a convenient form for applying the symmetric Strang splitting formula for the exponential operator [51–53]. Taking into account the separable form of the time-dependent potential,  $W(x, t) = U(x)\Sigma(t)$ , and taking advantage of the fact that each operator is unitarily equivalent to some multiplication operator owing to the adequate Fourier transform allows us to convert Eq. (16) into the following formula:

$$\begin{aligned} \varrho(x, p, t + \Delta t) &\approx \mathcal{F}_{1,\lambda \rightarrow x}^{-1} \exp \left( -\frac{i\Delta t}{2m} \lambda p \right) \mathcal{F}_{1,x \rightarrow \lambda} \\ &\quad \times \mathcal{F}_{2,y \rightarrow p}^{-1} \exp \left\{ i\Delta t \Sigma \left( t + \frac{\Delta t}{2} \right) \left[ U \left( x + \frac{y}{2} \right) \right. \right. \\ &\quad \left. \left. - U \left( x - \frac{y}{2} \right) \right] \right\} \mathcal{F}_{2,p \rightarrow y} \\ &\quad \times \mathcal{F}_{1,\lambda \rightarrow x}^{-1} \exp \left( -\frac{i\Delta t}{2m} \lambda p \right) \mathcal{F}_{1,x \rightarrow \lambda} \varrho(x, p, t), \end{aligned} \quad (17)$$

where the symbol  $\mathcal{F}_{a \rightarrow \alpha}$  denotes the ordinary Fourier transform and  $\mathcal{F}_{\alpha \rightarrow a}^{-1}$  corresponds to the inverse Fourier transform, while  $a$  and  $\alpha$  are a pair of the canonically conjugate variables. The physical meanings of such pairs  $(a, \alpha)$  are directly related

to the phase-space variables. The appropriate definitions and the derivation of the formula given by Eq. (17) can be found in Appendix A. The presented scheme can be further simplified if one considers the temporal part  $\Sigma(t)$  of the potential  $W(x, t)$  to be piecewise constant at some intervals  $[t_k, t_{k+1})$  with an amplitude  $A_k$ , namely, dividing the whole simulation time into

the intervals given by

$$[0, t_{\max}) = \bigcup_{k=0}^N [t_k, t_{k+1}). \quad (18)$$

In this way, one obtains the numerical algorithm for a single step of the time evolution of the WDF, expressed by the formula

$$\begin{aligned} \varrho(x, p, t_{k_{j+1}}) &\approx \mathcal{F}_{1,\lambda \rightarrow x}^{-1} \exp\left(-\frac{i\Delta t}{2m}\lambda p\right) \mathcal{F}_{1,x \rightarrow \lambda} \mathcal{F}_{2,y \rightarrow p}^{-1} \exp\left\{iA_k \Delta t \left[U\left(x + \frac{y}{2}\right) - U\left(x - \frac{y}{2}\right)\right]\right\} \\ &\times \mathcal{F}_{2,p \rightarrow y} \mathcal{F}_{1,\lambda \rightarrow x}^{-1} \exp\left(-\frac{i\Delta t}{2m}\lambda p\right) \mathcal{F}_{1,x \rightarrow \lambda} \varrho(x, p, t_{k_j}), \end{aligned} \quad (19)$$

where the subindex  $k_j$  stands for iteration within the interval  $[t_k, t_{k+1})$  in which  $\Sigma(t) = A_k$ .

### B. Entropic measures

A handy concept to describe quantum states in the phase space constitutes the Wigner-Rényi entropy because it provides information on the complexity of these states [39,41,54,55]. In particular, it enables one to describe the extension or shape of the state, which the WDF represents in the phase space. The sign problem of the WDF is not so severe in the case of pure states because the WDF corresponding to these states is interpreted as the probability density amplitude in the phase space according to the arguments presented in Ref. [56]. Hence, the squared modulus of the normalized WDF in the sense of the norm  $L^2(\mathbb{R}^2)$ , i.e.,  $\tilde{\varrho}(x, p, t) = \varrho(x, p, t)/\|\varrho(\cdot, \cdot, t)\|_{L^2(\mathbb{R}^2)}$ , is the proper probability density in the phase space [56], where  $\|\varrho(\cdot, \cdot, t)\|_{L^2(\mathbb{R}^2)} = (2\pi\hbar)^{-1/2}$ . The Wigner-Rényi entropy corresponding to the probability density,  $|\tilde{\varrho}(x, p, t)|^2$ , in the phase space for the Rényi index  $\alpha$ , where  $0 < \alpha < \infty$  and  $\alpha \neq 1$ , is defined as follows:

$$S_\alpha(t) = \frac{1}{1-\alpha} \ln \left\{ (2\pi\hbar)^{\alpha-1} \int_{\mathbb{R}^2} dx dp [|\tilde{\varrho}(x, p, t)|^2]^\alpha \right\}, \quad (20)$$

whereby, between the Wigner-Rényi entropies corresponding to different Rényi indexes  $\alpha$  and  $\alpha'$ , there is the inequality  $S_\alpha(t) > S_{\alpha'}(t)$  for  $\alpha < \alpha'$  and a fixed time  $t$ , as demonstrated in Appendix B. The attractive property of the Wigner-Rényi entropy is their relation to the Hartley entropy [57], the Wigner-Rényi's one-half [41], the Shannon entropy [39], the collision entropy [38], and the min-entropy [58] for the Rényi index, which equal  $\alpha = 0, 1/2, 1, 2, \infty$ , respectively. Let us note that the Wigner-Rényi entropies for different Rényi indexes can be regarded as examples of the symplectically invariant measures, by Eqs. (6) and (7). This observation plays a crucial role in the presented research. Here we focus our attention on only four of the previously mentioned entropies, defined up to a constant  $\ln(1/2\pi\hbar)$ , namely, the Wigner-Rényi's one-half entropy, which is given by the formula

$$S_{1/2}(t) = 2 \ln \left[ \int_{\mathbb{R}^2} dx dp |\tilde{\varrho}(x, p, t)| \right], \quad (21)$$

the Shannon entropy which is given by the formula

$$\begin{aligned} S_1(t) &= \lim_{\alpha \rightarrow 1} S_\alpha(t) = -2 \int_{\mathbb{R}^2} dx dp \\ &\times |\tilde{\varrho}(x, p, t)|^2 \ln [|\tilde{\varrho}(x, p, t)|^2], \end{aligned} \quad (22)$$

the collision entropy which is given by the formula

$$S_2(t) = -\ln \int_{\mathbb{R}^2} dx dp |\tilde{\varrho}(x, p, t)|^4, \quad (23)$$

and last but not least, the min-max entropy,

$$\begin{aligned} S_\infty(t) &= \lim_{\alpha \rightarrow +\infty} \frac{1}{1-\alpha} \ln \left\{ \int_{\mathbb{R}^2} dx dp [|\tilde{\varrho}(x, p, t)|^2]^\alpha \right\} \\ &= -\ln \left[ \max_{(x,p) \in \mathbb{R}^2} |\tilde{\varrho}(x, p, t)|^2 \right]. \end{aligned} \quad (24)$$

All of them have precise physical meanings. The Wigner-Rényi's one-half entropy is related to the area occupied by the negative part of the WDF in the phase space [41], and the Shannon entropy is associated with a deformation of the area occupied by the WDF in phase space caused by the quantum correlations of momentum position, which simultaneously influence the shape of this function. In turn, collision entropy is related to the inverse participation ratio in the phase space [59]. Last but not least, the min-max entropy is related to the maximum of the probability density over the phase space. The symplectic invariance of Rényi entropic measures is the essential property in defining the interaction time  $\tau$  between the quantum state represented by the function  $\varrho(x, p, t)$  and the potential  $W(x, t)$ . First of all, notice that at any given time  $t$  during the interaction with the absolutely integrable barrier-well potential, it cannot be approximated with good precision by a single polynomial of the order of, at most, 2 in the whole subset of  $\mathbb{R}$ , where the marginal distribution of the considered quantum state in the position space,

$$n(x, t) = \int_{\mathbb{R}} dp \varrho(x, p, t), \quad (25)$$

is noticeably nonzero. Hence, during the interaction with the potential, the time evolution of the WDF is nonsymplectic. Consequently, we expect that the Rényi entropy will be non-constant during that time. However, away from the potential



center, the motion of the WDF can be regarded as a free propagation. As we have previously shown, this kind of evolution acts as a shearing transformation of the WDF [see Eq. (10)], leaving symplectically invariant measures constant, as implied by Eq. (7). Hence, during free propagation of the WDF, the Rényi entropy is constant. The beginning of the interaction  $t_i$  can be understood as an instance when WDF starts to interact with the potential and, consequently, a first visible change in the symplectically invariant measure occurs. Complementary to that,  $t_f$  is the time associated with the end of the interaction, when the WDF evolves freely, which results in stabilization of the symplectically invariant measure. Both instances are measured indirectly. They require a measuring device with given precision  $\varepsilon$  to detect the first and last changes in the evolution of the symplectically invariant measure. We have encapsulated our physical reasoning within the following definition:

**Definition 1.** For a fixed Rényi index  $\alpha > 0$ , the interaction time  $\tau$  between the state represented by the Wigner distribution function and potential energy belonging to the class of absolutely integrable functions, based upon Wigner-Rényi entropic measure, can be defined as

$$\begin{aligned} \tau &= \min\{t \in \mathbb{R}_+ : |S_\alpha(t) - S_\alpha(\infty)| > \varepsilon(M - m)\} \\ &\quad - \max\{t \in \mathbb{R}_+ : |S_\alpha(t) - S_\alpha(0)| > \varepsilon(M - m)\} \\ &= t_f - t_i, \end{aligned} \quad (26)$$

where  $S_\alpha(t)$  is a Wigner-Rényi entropy with Rényi index  $\alpha$ ,  $S_\alpha(0)$  is the value of the entropy at the beginning of the evolution,  $S_\alpha(\infty)$  is the value at the end of the evolution,  $M = \max_{t \in \mathbb{R}_+} S_\alpha(t)$  is the maximum of the Wigner-Rényi entropic measure,  $m = \min_{t \in \mathbb{R}_+} S_\alpha(t)$  is its minimum, and  $0 < \varepsilon \ll 1$  is a dimensionless threshold parameter that can be understood as the precision of the measuring device.

The infinity that is present in the definition is treated as a time that is long enough so that the evolution after the interaction is that of a free particle, as usually taken in scattering theory. In the case of the numerical experiment, this is the time of the simulation. Ideally,  $S_\alpha(0)$ ,  $S_\alpha(\infty)$  should be known *a priori* so that a threshold comparison could be made on the go rather than after the experiment.

### III. RESULTS AND DISCUSSION

The quantitative description of the quantum state scattering requires specification of the potential term of the system Hamiltonian, which represents the scatterer. We model this scatterer using a time-dependent finite-range potential with a periodically changing amplitude. For this purpose, we use a locally integrable function which allows us to determine the effective interaction region and the interaction time according to Definition 1. The results of all numerical calculations are presented in atomic units (a.u.), i.e.,  $e = \hbar = m = 1$ .

In the presented study, we assume that the potential term  $W(x, t) = U(x)\Sigma(t)$  of the Weyl symbol of the effective Hamiltonian (1) consists of the spatial term

$$U(x) = U_0 \exp\left[-\frac{(x - x_B)^2}{2w^2}\right], \quad (27)$$

representing a scattering center of strength  $U_0 = 0.008$  a.u. localized at  $x_B = 0$  a.u. and with width given by  $w^2 = 50$  a.u., and the time-dependent term

$$\Sigma(t) = \theta(t_b - t) + \text{sgn}\left[\sin \frac{2\pi(t - t_b)}{T}\right] \theta(t - t_b) \quad (28)$$

responsible for oscillations between the barrier regime and the well regime. These oscillations start after the delay time  $t_b = 140$  a.u., and their rate is given by the period  $T$  which is a parameter of the model. Therefore, the choice of this parameter remains critical for studying the dynamics of the quantum state during its interaction with the time-varying obstacle represented by the periodic potential in the form given by Eqs. (27) and (28). Our proposition of determining the reasonable value of  $T$  is partially based on a measure of the similarity of two states resulting from the Hilbert-Schmidt distance definition [60], which can be expressed in terms of the WDF as follows:

$$\begin{aligned} d_{\varrho, \varrho_0}(t) &= \left\{ 2\pi\hbar \int_{\mathbb{R}^2} dx dp \left[ \varrho(x, p, t) - \varrho_0\left(x - \frac{p}{m}t, p\right) \right]^2 \right\}^{1/2} \\ &= \sqrt{2} [1 - c_{\varrho, \varrho_0}(t)]^{1/2}, \end{aligned} \quad (29)$$

where the dynamic overlap measure  $c_{\varrho, \varrho_0}(t)$  is expressed by the formula

$$c_{\varrho, \varrho_0}(t) = 2\pi\hbar \int_{\mathbb{R}^2} dx dp \varrho(x, p, t) \varrho_0\left(x - \frac{p}{m}t, p\right), \quad (30)$$

in which  $\varrho_0(x - pt/m, p)$  corresponds to the free-space dynamics of the WDF. In turn, the time dependence of the function  $\varrho(x, p, t)$  results from the numerical solution of the Cauchy problem (3) for the Moyal equation with a fixed period  $T$  and with the initial condition given by the coherent superposition of two well-separated Gaussians,

$$\begin{aligned} \varrho_0(x, p) &= A_1^2 \frac{(1 - \beta)}{\pi\hbar} \exp\left[-\frac{(x - x_1)^2}{2\delta_x^2} - \frac{2\delta_x^2(p - p_0)^2}{\hbar^2}\right] \\ &\quad + A_1^2 \frac{\beta}{\pi\hbar} \exp\left[-\frac{(x - x_2)^2}{2\delta_x^2} - \frac{2\delta_x^2(p - p_0)^2}{\hbar^2}\right] \\ &\quad + 2A_1^2 \frac{\sqrt{\beta(1 - \beta)}}{\pi\hbar} \cos\left[\vartheta + \frac{p - p_0}{\hbar}(x_1 - x_2)\right] \\ &\quad \times \exp\left[-\frac{(x - \frac{x_1 + x_2}{2})^2}{2\delta_x^2} - \frac{2\delta_x^2(p - p_0)^2}{\hbar^2}\right], \end{aligned} \quad (31)$$

where the normalization factor  $A_1$  has the form

$$A_1 = \left[ 1 + 2\sqrt{\beta(1 - \beta)} \exp\left(-\frac{(x_1 - x_2)^2}{8\delta_x^2}\right) \right]^{-\frac{1}{2}}. \quad (32)$$

The set of parameters defining this bimodal WDF is taken in the same form as in our previous work [61] for the quality parameter  $\Gamma = 1$ , namely,  $\beta = 0.5$ ,  $\vartheta = 0$ ,  $\delta_x^2 = 500$  a.u.,  $x_1 = -300$  a.u.,  $x_2 = -500$  a.u., and  $p_0 = 0.15$  a.u. In fact, the WDF given by Eq. (31) is the phase-space representation of the Schrödinger cat state [62]. Based on the solution of the Cauchy problem mentioned above with the initial condition in the form given by Eq. (31), we can determine the dynamic overlap measure,  $c_{\varrho, \varrho_0}(t)$  because we also know the free-space

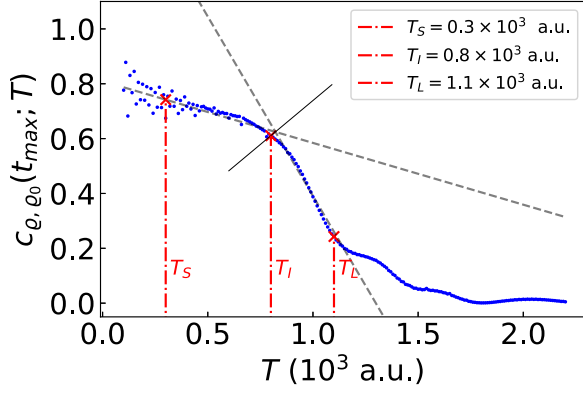


FIG. 1. Long-time dynamic overlap measure as a function of period  $T$ . The continuous gray line is the bisector of the angle between two gray dashed lines, which approximate the behavior at a short period interval and intermediate period interval. Red crosses stand for representatives which abscissas were taken for further analysis.

propagation form of the WDF,  $\varrho_0(x - pt/m, p)$ , with the same initial condition. However, let us note that this specified

quantity parametrically depends on  $T$ , i.e.,  $c_{\varrho, \varrho_0}(t) = c_{\varrho, \varrho_0}(t; T)$ . To determine the values of the potential period, we calculate the dynamic overlap measure,  $c_{\varrho, \varrho_0}(t; T)$ , as a function of the period  $T$ , for a fixed value of  $t = t_{\max}$ . Specifically, at a fixed time  $t_{\max} = 8.5 \times 10^3$  a.u., corresponding to the maximum of the simulation time, this measure assesses the degree to which the propagating WDF deviates from the free-space propagation after interaction with the potential  $W(x, t)$  within the prescribed potential period  $T$ , as presented in Fig. 1.

The disparities in the evolution of the quantum state in different configurations of the system are clearly visible: as  $T$  tends to zero, a substantial overlap (exceeding 80%) emerges between the free-propagating WDF and that confined within the rapidly oscillating potential  $T$ . The trend was followed by a predominant decrease in the measure, approaching nearly zero for  $T$  exceeding  $1.7 \times 10^3$  a.u., indicating that the states are fundamentally distinct. The red line in the figure demarcates the characteristic period timescales  $T_S$ ,  $T_I$  and the transitional timescale  $T_L$ . We refer to these scales as short (S), intermediate (I), and long (L). As a first step, we

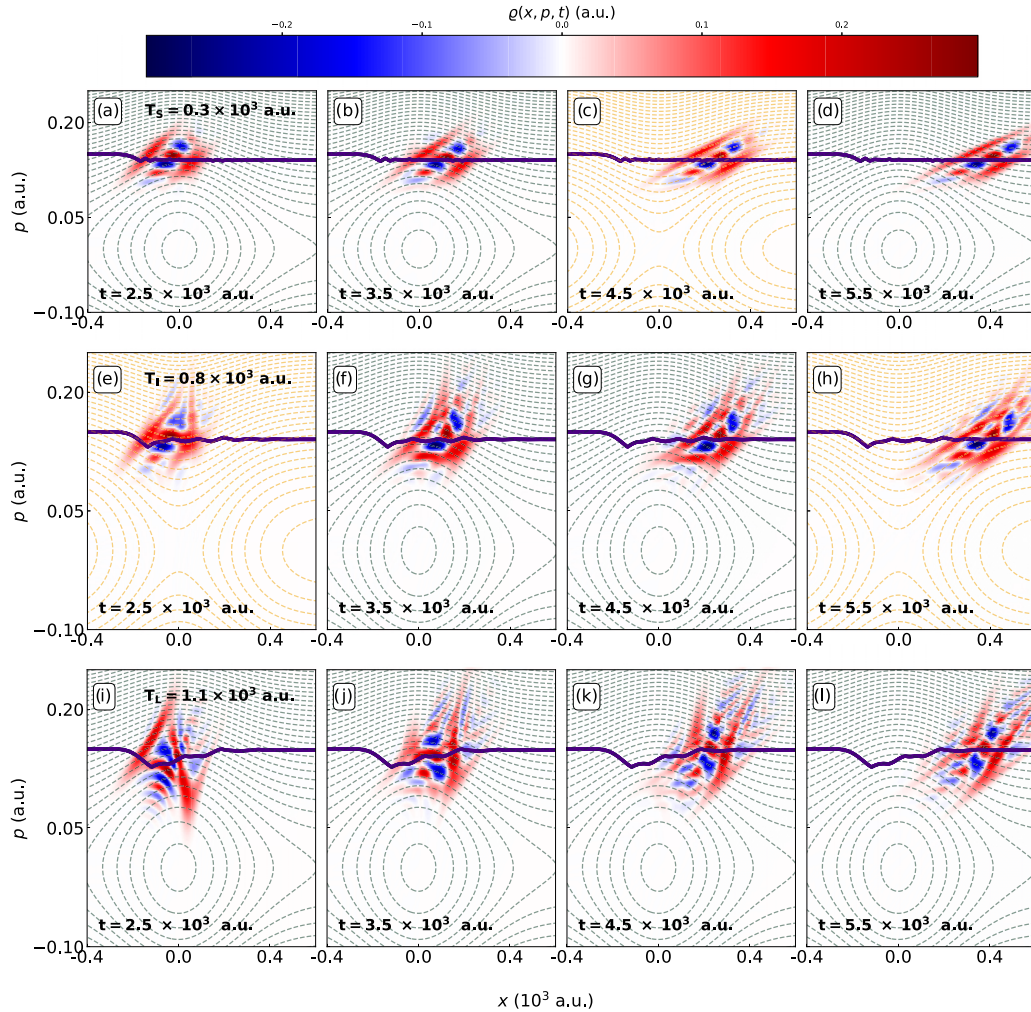


FIG. 2. The phase-space snapshots of the WDF taken at  $t = 2.5 \times 10^3$  a.u.,  $3.5 \times 10^3$  a.u.,  $4.5 \times 10^3$  a.u., and  $5.5 \times 10^3$  a.u. (columns) for different potential periods  $T \in \{T_S, T_I, T_L\}$  (rows). The dashed lines stand for the phase-space portrait of the Weyl symbol of the Hamiltonian, whereas the solid purple line is the quantum trajectory of the WDF.

investigate the influence of the potential periods  $\{T_S, T_I, T_L\}$  on the dynamics of the WDF. The results of the calculation are presented in Fig. 2 where the phase-space snapshots and quantum trajectories are displayed.

Undoubtedly, the dynamics of WDF depends on the period  $T$  of the modulator  $\Sigma(t; T)$ . With an increasing period, the time of interaction with the fixed state of the potential  $U(x)$  increases. The rapid oscillating barrier ( $T = T_S$ ), presented in Figs. 2(a)–2(d), almost does not disturb the evolution. The general influence of the potential can be noticed in the quantum trajectory, namely, a cusp associated with a diminished value of the average momentum. This effect is more visible in the next cases where periodic changes of the character are not as frequent. In addition to reducing the momentum of the WDF, its shape is also mutilated. By leveraging our understanding of the dynamics of the WDF, we determine the time-dependent Wigner-Rényi's entropies,  $S_{1/2}(t)$ ,  $S_1(t)$ ,  $S_2(t)$ ,  $S_\infty(t)$ , which are examples of the symplectically invariant quantities. Furthermore, through these functions, we can estimate the interaction time, drawing on the insights highlighted in Definition 1. The results of the calculations are presented in Fig. 3 for different potential periods  $T$ . According to Fig. 3, all Wigner-Rényi  $\alpha$  entropies, for  $\alpha \in \{1/2, 1, 2, \infty\}$ , exhibit three distinct regions of evolution. Namely, they are constant for the initial evolution of the WDF, then they start rapidly evolving in a nonmonotone manner, suggesting the ongoing interaction, finalized by yet again constant value. It is worth mentioning that for fixed  $\alpha$ , the  $S_\alpha(t)$  attains higher values in a long-time evolution for increasing values of the potential period  $T$ :  $S_\alpha(t_{\max}; T_S) < S_\alpha(t_{\max}; T_I) < S_\alpha(t_{\max}; T_L)$ . For a fixed  $T$ , the evolution of the Wigner-Rényi entropies of various orders, namely,  $S_{1/2}(t)$ ,  $S_1(t)$ ,  $S_2(t)$ , and  $S_\infty(t)$ , exhibit a consistent ordering such that  $S_\infty(t)$  serves as the lower bound, while  $S_{1/2}(t)$  is the upper bound, with  $S_1(t)$  and  $S_2(t)$  positioned in between, namely,  $S_{1/2}(t) > S_1(t) > S_2(t) > S_\infty(t)$ . Regardless of the value of the modulator period  $T$ , the long-time behavior of all these measures is approximately constant, rendering Definition 1 a valid method to determine the interaction time between the WDF and the potential  $W(x, t)$ . The estimated interaction times for  $\varepsilon = 0.01$  are shown in Fig. 4. Generally, the interaction time as a function of  $T$  exhibits a decreasing trend as  $T$  increases. For  $T \ll 1 \times 10^3$  a.u., the character of the evolution is similar to that of free motion due to rapid oscillations of the barrier, resulting in mutual cancellation of the effects characteristic to the interaction with potential barrier and well. Moreover, for  $T > 0.5 \times 10^3$  a.u., the interaction time  $\tau(T)$  resembles a reverse ordering in comparison to the Wigner-Rényi entropies in Fig. 3. Namely, the interaction time  $\tau$  based on the Wigner-Rényi one-half entropy  $S_{1/2}(t)$  yields a lower bound for the family of interaction times. We leverage two physical measures, i.e., dynamical capture and transmission coefficients, to validate the reliability of our proposition. These measures are not symplectically invariant, but their straightforward physical interpretation helps to assess whether our results align with the expected patterns, as shown in Figs. 3 and 4. The simplicity in their interpretation makes them valuable tools; in particular, they can serve as complementary measures to estimate the interaction time of the considered model. The dynamical capture coefficient,

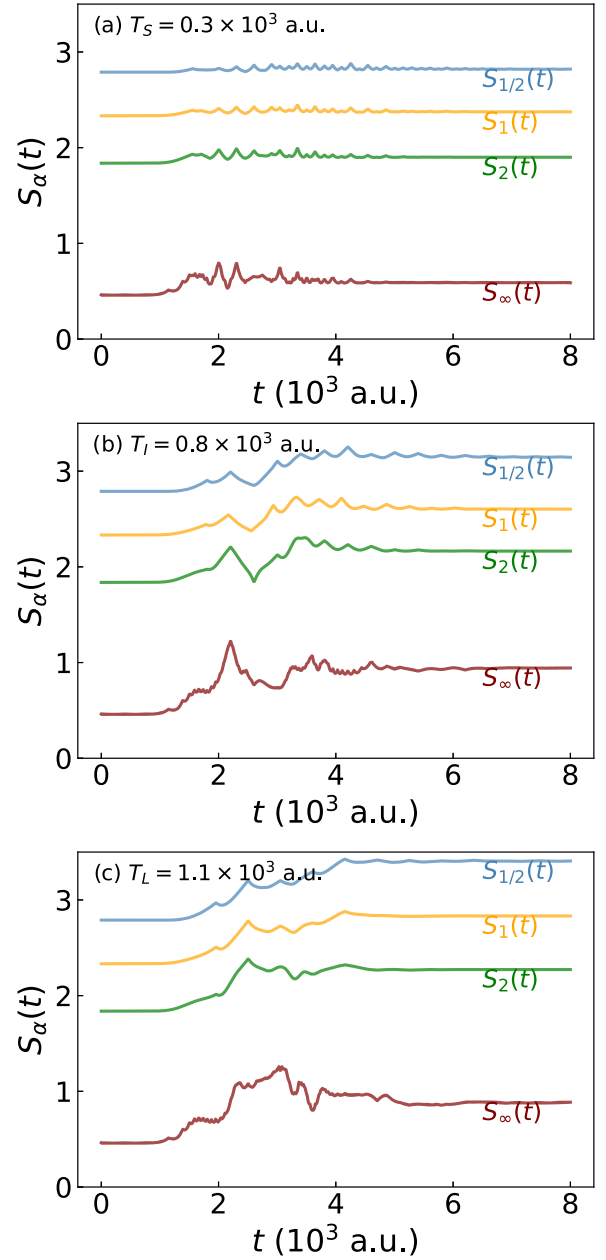


FIG. 3. The comparison between different entropic measures for  $\alpha \in \{1/2, 1, 2, \infty\}$  for different potential periods (a) short, (b) intermediate, and (c) long.

defined as

$$C(t) = \int_{\mathbb{R}} \int_L dx dp \varrho(x, p, t), \quad (33)$$

where  $L$  is an interval containing the maximum of considered potential, quantifies the amount of the WDF within the potential  $U(x)$ . Complementary dynamical transmission coefficient

$$P(t) = \int_{\mathbb{R}} \int_{x_p}^{\infty} dx dp \varrho(x, p, t) \quad (34)$$

measures the amount of transmitted WDF. These coefficients satisfy the limit condition  $\lim_{t \rightarrow +\infty} [R(t) + C(t) + P(t)] = 1$ , where  $R(t)$  is the dynamical reflection coefficient. The traits



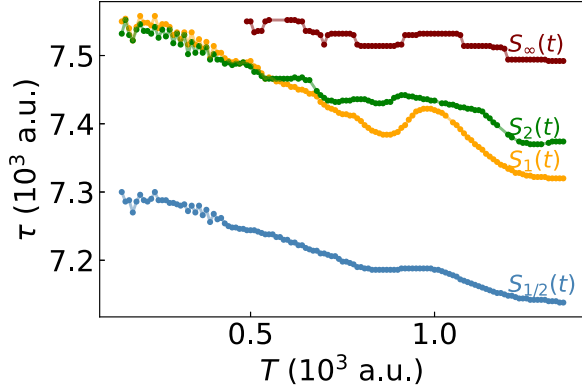


FIG. 4. The interaction time  $\tau$  based upon different entropic measures  $S_\alpha(t)$  for  $\alpha \in \{1/2, 1, 2, \infty\}$ . The results for  $S_\infty(t)$  when  $T < 0.5 \times 10^3$  a.u. were dropped as our method could not provide results smaller than the simulation time.

of the evolution of the WDF are captured in Figs. 5(a) and 5(b). The dynamical capture coefficient  $C(t)$  quantifies the localization of WDF around the peak value of the Gaussian potential, while the dynamical transmission coefficient  $P(t)$  provides the amount of the WDF that traversed a specific region of the space, distant from the potential. In the presented case,  $C(t)$  starts to vary after the period of stagnation (where none of the WDF is currently interacting with the potential for

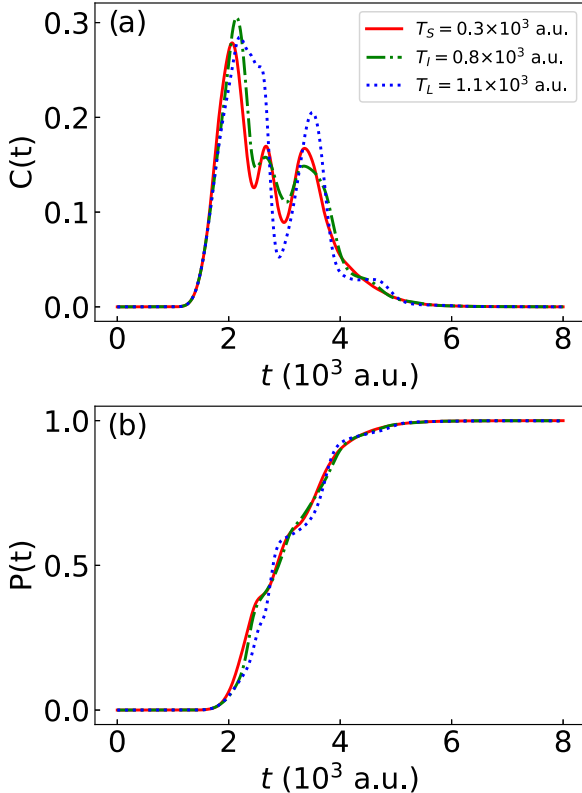


FIG. 5. (a) Dynamical capture  $C$  and (b) dynamical transmission  $P$  coefficients as functions of time  $t$ . The colored curves represent different periods  $T$  of potential  $U(x; T)$ : short  $T_S$ , intermediate  $T_I$ , and long  $T_L$ .

$t < t_1$ ). This interaction is followed by another time interval where  $C(t) = 0$  for  $t > t_2$ . Generally, one could approach the problem of estimating the interaction time between the WDF and the potential purely on the basis of the distance between consecutive intervals where  $C(t) = 0$ , namely,  $t_2 - t_1$ . However, this approach does not align with the interaction time proposed in Definition 1, as it relies on the WDF's presence within a specific spatial interval, rather than the character of the evolution. In this context, the free evolution of the state serves as a natural indicator of the end of the interaction between the WDF and the potential. Crucially, the WDF exits the interaction zone in all presented cases of  $T$  [Fig. 5(a)]. This implies that irrespective of the interaction's nature, no WDF accumulates near the potential maximum. However, it does not necessarily imply that the WDF is no longer interacting. In particular, the hypothetical interaction time based on the dynamical capture coefficient results in a single value for all possible variations of the parameter  $T$  [as seen in Fig. 5(b)], which is in contradiction to the result presented in Fig. 4.

#### IV. CONCLUSIONS AND DISCUSSION

We have used the symplectic invariance property of the time-dependent family of the Wigner-Rényi entropies of the order of one-half, 1, 2, and  $\infty$  to estimate the interaction time between a periodically driven system and a quantum state. The presented results have been achieved from the numerical solution of the Moyal equation with the initial condition in the form of the Schrödinger cat state for the driven system with the model of the time-dependent potential term in the separable form. Based on analyzing a dynamic overlap measure in the long-time regime, we selected three distinct potential periods, i.e., short, intermediate, and long, to represent different evolution traits of the considered state. Numerical analysis has revealed a descending order of the entropies, with the one-half Wigner-Rényi entropy as the upper limit and the Wigner-Rényi min-max entropy as the lower limit, which analytical calculations have supported. Furthermore, adequate entropy exhibited a higher long-term value with an increasing potential period for a fixed value of the Rényi index. The considered entropies demonstrate a nearly constant behavior, both at the initiation and finalization of the simulation, facilitating the estimation of the interaction time, as outlined by our Definition. By calculating the difference between two distinct time instances that mark the beginning and end of the interaction, we estimated the duration of the interaction between the state and the potential. Interestingly, the interaction time exhibited reverse ordering compared to the entropies, with one-half Wigner-Rényi entropy now serving as a lower bound. In addition, we have observed that as the intensity of the oscillations equivalently increased, the potential period was lowered and the strength of the interaction between the state and the potential increased, resulting in a longer exposure of the state to the deformations provided by the barrier.

#### ACKNOWLEDGMENT

The research project is supported by the program “Initiative for Excellence – Research University” for the AGH University of Krakow.



### APPENDIX A: ALGORITHM FOR SOLVING MOYAL EQUATION WITH TIME-DEPENDENT POTENTIALS

Here, we will derive the formula used for calculating the Wigner distribution function (WDF) for the time-dependent potential. According to Eq. (4), the Moyal operator can be written symbolically as  $-i\hat{\mathcal{L}}_M(t)$ . The formal solution, for an initial condition in the form  $\varrho_0(x, p)$ , is given by

$$\varrho(x, p, t) = \mathcal{T} e^{-i \int_0^t ds \hat{\mathcal{L}}_M(s)} \varrho_0(x, p), \quad (\text{A1})$$

where  $\mathcal{T}$  is Dysons' time-ordering operator. The exponential present in the above equation is crucial for describing the time evolution at any time instance  $t + \Delta t$ , for some time interval  $\Delta t > 0$ . In this case, it can be substituted by the following relation [50]:

$$\mathcal{T} e^{-i \int_t^{t+\Delta} ds \hat{\mathcal{L}}_M(s)} = \exp\{\Delta t[-i\hat{\mathcal{L}}_M(t) + \hat{D}]\}, \quad (\text{A2})$$

where the operator  $\hat{D}$  was defined in Eq. (15). This gives the equivalent expression for calculating the WDF at an instance  $t + \Delta t$ ,

$$\begin{aligned} \varrho(x, p, t + \Delta t) &= \mathcal{T} e^{-i \int_t^{t+\Delta} ds \hat{\mathcal{L}}_M(s)} \varrho(x, p, t) \\ &= e^{\Delta t(-i\hat{\mathcal{L}}_M(t) + \hat{D})} \varrho(x, p, t). \end{aligned} \quad (\text{A3})$$

Substituting the form of the operator  $-i\hat{\mathcal{L}}_M(t)$  into the expression above yields

$$\varrho(x, p, t + \Delta t) = e^{\Delta t(\hat{T} + \hat{U}(t) + \hat{D})} \varrho(x, p, t), \quad (\text{A4})$$

where  $\hat{T}$  is a kinetic energy operator,

$$\hat{T} = -\frac{p}{m} \partial_x, \quad (\text{A5})$$

and, complementary to that,  $\hat{U}(t)$  is the time-dependent potential energy operator,

$$\hat{U}(t) = \frac{1}{i\hbar} \Sigma(t) \left[ U\left(x + \frac{i\hbar}{2} \partial_p\right) - U\left(x - \frac{i\hbar}{2} \partial_p\right) \right]. \quad (\text{A6})$$

For further manipulations, one must agree upon an approximation of the exponential expression or, in other words, splitting of the exponential. One of such methods is the Strang approximation [51] of the second order, for the operators  $\hat{T} + \hat{D}$ , and  $\hat{U}(t)$ , according to which

$$\varrho(x, p, t + \Delta t) \approx e^{\frac{\Delta t}{2}(\hat{T} + \hat{D})} e^{\Delta t \hat{U}(t)} e^{\frac{\Delta t}{2}(\hat{T} + \hat{D})} \varrho(x, p, t). \quad (\text{A7})$$

Furthermore, per [50], the operators  $\hat{T}$  and  $\hat{D}$  commute, resulting in

$$\varrho(x, p, t + \Delta t) \approx e^{\frac{\Delta t}{2} \hat{T}} e^{\Delta t \hat{U}(t + \Delta t/2)} e^{\frac{\Delta t}{2} \hat{T}} \varrho(x, p, t). \quad (\text{A8})$$

To omit the difficulties related to the evaluation of the exponential differential operator and to perform numerical calculations, we introduce the following Fourier transforms:

$$\mathcal{F}_{1,x \rightarrow \lambda} \varrho(x, p, t) = \frac{1}{\sqrt{2\pi\hbar}} \int_{\mathbb{R}} dx e^{-\frac{i}{\hbar} \lambda x} \varrho(x, p, t), \quad (\text{A9})$$

$$\mathcal{F}_{1,\lambda \rightarrow x}^{-1} \varrho(\lambda, p, t) = \frac{1}{\sqrt{2\pi\hbar}} \int_{\mathbb{R}} d\lambda e^{\frac{i}{\hbar} \lambda x} \varrho(\lambda, p, t), \quad (\text{A10})$$

$$\mathcal{F}_{2,p \rightarrow y} \varrho(x, p, t) = \frac{1}{\sqrt{2\pi\hbar}} \int_{\mathbb{R}} dp e^{-\frac{i}{\hbar} p y} \varrho(x, p, t), \quad (\text{A11})$$

$$\mathcal{F}_{2,y \rightarrow p}^{-1} \varrho(x, y, t) = \frac{1}{\sqrt{2\pi\hbar}} \int_{\mathbb{R}} dy e^{\frac{i}{\hbar} p y} \varrho(x, y, t) dy, \quad (\text{A12})$$

and we use the unitary equivalence between the derivative and multiplicative operators. As a result, the following algorithm for numerical calculation of the time evolution of the WDF in time-dependent potentials arises:

$$\begin{aligned} \varrho(x, p, t_0 + \Delta t) &\approx \mathcal{F}_{1,\lambda \rightarrow x}^{-1} \exp\left(-\frac{i\Delta t}{2m} \lambda p\right) \mathcal{F}_{1,x \rightarrow \lambda} \mathcal{F}_{2,y \rightarrow p}^{-1} \exp\left\{i\Delta t \Sigma\left(t_0 + \frac{\Delta t}{2}\right) \left[U\left(x + \frac{y}{2}\right) - U\left(x - \frac{y}{2}\right)\right]\right\} \mathcal{F}_{2,p \rightarrow y} \mathcal{F}_{1,\lambda \rightarrow x}^{-1} \\ &\times \exp\left(-\frac{i\Delta t}{2m} \lambda p\right) \mathcal{F}_{1,x \rightarrow \lambda} \varrho(x, p, t_0). \end{aligned} \quad (\text{A13})$$

### APPENDIX B: MONOTONE DECREASE OF WIGNER-RÉNYI ENTROPIES

Let  $f(x, p, t) = \tilde{\varrho}^2(x, p, t)$  be a probability distribution function over a phase space generated by  $(x, p)$  variables for all  $t$ . We will show that the Wigner-Rényi entropy of the order  $\alpha \geq 0$  satisfies the following inequality:

$$S_\alpha(t) \leq S_\beta(t), \quad \alpha \geq \beta. \quad (\text{B1})$$

To see this, first, we calculate the derivative of  $S_\alpha(t)$  with respect to the parameter  $\alpha$ . This gives

$$\partial_\alpha S_\alpha(t) = \frac{1}{(1-\alpha)^2} \ln \left[ \int_{\mathbb{R}^2} dx dp f^\alpha(x, p, t) \right] + \frac{1}{1-\alpha} \left[ \int_{\mathbb{R}^2} dx dp f^\alpha(x, p, t) \right]^{-1} \int_{\mathbb{R}^2} dx dp f^\alpha(x, p, t) \ln f(x, p, t). \quad (\text{B2})$$

Now, introducing new quantities: the  $\alpha$ th power of the phase-space  $\alpha$ -norm of  $f(x, p, t)$ ,

$$N_\alpha(t) := \int_{\mathbb{R}^2} dx dp f^\alpha(x, p, t), \quad (\text{B3})$$

and the normalized probability distribution,

$$q_\alpha(x, p, t) := \frac{1}{N_\alpha(t)} f^\alpha(x, p, t), \quad (\text{B4})$$

where

$$\int_{\mathbb{R}^2} dx dp q_\alpha(x, p, t) = 1, \quad (\text{B5})$$

one may rewrite

$$\partial_\alpha S_\alpha(t) = \frac{1}{(1-\alpha)^2} \ln N_\alpha(t) - \frac{1}{(1-\alpha)^2} \int_{\mathbb{R}^2} dx dp q_\alpha(x, p, t) \ln f^{\alpha-1}(x, p, t). \quad (\text{B6})$$

Performing some manipulation regarding the logarithmic expression, we get

$$\ln f^{\alpha-1}(x, p, t) = \ln \left[ \frac{f^\alpha(x, p, t)}{N(t)} \frac{N_\alpha(t)}{f(x, p, t)} \right] = \ln \left[ q_\alpha(x, p, t) \frac{N_\alpha(t)}{f(x, p, t)} \right] = \ln \left[ \frac{q_\alpha(x, p, t)}{f(x, p, t)} \right] + \ln N(t). \quad (\text{B7})$$

This yields the following expression:

$$\partial_\alpha S_\alpha(t) = \frac{1}{(1-\alpha)^2} \ln N_\alpha(t) - \frac{1}{(1-\alpha)^2} \int_{\mathbb{R}^2} dx dp q_\alpha(x, p, t) \ln \frac{q_\alpha(x, p, t)}{f(x, p, t)} - \frac{\ln N_\alpha(t)}{(1-\alpha)^2}, \quad (\text{B8})$$

equal to

$$\partial_\alpha S_\alpha(t) = -\frac{1}{(1-\alpha)^2} \int_{\mathbb{R}^2} dx dp q_\alpha(x, p, t) \ln \frac{q_\alpha(x, p, t)}{f(x, p, t)} = -\frac{1}{(1-\alpha)^2} \int_{\mathbb{R}^2} dx dp q_\alpha(x, p, t) \ln \frac{q_\alpha(x, p, t)}{\tilde{q}^2(x, p, t)}, \quad (\text{B9})$$

which is a relative entropy [Kullback-Leiber divergence  $D_{KL}(q_\alpha, \tilde{q}^2)$ ] of the probability distribution functions  $q_\alpha(x, p, t)$  and  $\tilde{q}^2(x, p, t)$  that is non-negative [63],

$$D_{KL}(q_\alpha, \tilde{q}^2) \geq 0 \Rightarrow \partial_\alpha S_\alpha(t) \leq 0, \quad (\text{B10})$$

and thus  $S_\alpha(t) \leq S_\beta(t)$ ,  $\alpha \geq \beta$ . This property holds for any positive function  $f \in L^1(\mathbb{R}^2, dx dp) \cap L^\alpha(\mathbb{R}^2, dx dp)$ .

- 
- [1] T. Dittrich, P. Hänggi, G.-L. Ingold, B. Kramer, G. Schön, and W. Zwerger, *Quantum Transport and Dissipation* (Wiley-Vch, Weinheim, 1998), Vol. 3.
- [2] A. Kenfack, J. Gong, and A. K. Pattanayak, *Phys. Rev. Lett.* **100**, 044104 (2008).
- [3] C. Grossert, M. Leder, S. Denisov, P. Hänggi, and M. Weitz, *Nat. Commun.* **7**, 10440 (2016).
- [4] P. Hänggi and F. Marchesoni, *Rev. Mod. Phys.* **81**, 387 (2009).
- [5] P. Olbrich, J. Karch, E. L. Ivchenko, J. Kamann, B. März, M. Fehrenbacher, D. Weiss, and S. D. Ganichev, *Phys. Rev. B* **83**, 165320 (2011).
- [6] H. R. Reiss, *Phys. Rev. Lett.* **25**, 1149 (1970).
- [7] J. C. Bronski, L. D. Carr, B. Deconinck, J. N. Kutz, and K. Promislow, *Phys. Rev. E* **63**, 036612 (2001).
- [8] T. Wang, N. F. Q. Yuan, and L. Fu, *Phys. Rev. X* **11**, 021024 (2021).
- [9] M. Khazali, *Quantum* **6**, 664 (2022).
- [10] K. Sacha and J. Zakrzewski, *Rep. Prog. Phys.* **81**, 016401 (2018).
- [11] M. Holthaus, *J. Phys. B: At. Mol. Opt. Phys.* **49**, 013001 (2016).
- [12] S. Blanes, F. Casas, J. A. Oteo, and J. Ros, *Phys. Rep.* **470**, 151 (2009).
- [13] J. Weinbub and D. K. Ferry, *Appl. Phys. Rev.* **5**, 041104 (2018).
- [14] W. P. Schleich, *Quantum Optics in Phase Space* (Wiley, New York, 2001).
- [15] M. A. Alonso, *Adv. Opt. Photon.* **3**, 272 (2011).
- [16] U. Chabaud, P.-E. Emeriau, and F. Grosshans, *Quantum* **5**, 471 (2021).
- [17] R. Raussendorf, C. Okay, M. Zurel, and P. Feldmann, *Quantum* **7**, 979 (2023).
- [18] L. Kocia and P. Love, *Quantum* **5**, 494 (2021).
- [19] T. J. H. Hele, M. J. Willatt, A. Muolo, and S. C. Althorpe, *J. Chem. Phys.* **142**, 134103 (2015).
- [20] W. Xie, W. Domcke, S. C. Farantos, and S. Y. Grebenshchikov, *J. Chem. Phys.* **144**, 104105 (2016).
- [21] A. Montoya-Castillo and D. R. Reichman, *J. Chem. Phys.* **146**, 024107 (2017).
- [22] L. Slocombe, M. Sacchi, and J. Al-Khalili, *Commun. Phys.* **5**, 109 (2022).
- [23] H. Warman, L. Slocombe, and M. Sacchi, *RSC Adv.* **13**, 13384 (2023).
- [24] B. Opanchuk and P. D. Drummond, *J. Math. Phys.* **54**, 042107 (2013).
- [25] K. Kirkpatrick, A. E. Mirasola, and C. Prescod-Weinstein, *Phys. Rev. D* **102**, 103012 (2020).
- [26] J. Su, H. Lyu, and Y. Zhang, *Phys. Lett. A* **443**, 128218 (2022).
- [27] J. Bera, B. Halder, S. Ghosh, R.-K. Lee, and U. Roy, *Phys. Lett. A* **453**, 128484 (2022).
- [28] P. Massignan, A. Lampo, J. Wehr, and M. Lewenstein, *Phys. Rev. A* **91**, 033627 (2015).
- [29] S. Lally, N. Werren, J. Al-Khalili, and A. Rocco, *Phys. Rev. A* **105**, 012209 (2022).
- [30] A. A. Valido, *J. Stat. Mech.* (2022) 073103.
- [31] M. A. Prado Reynoso, P. C. López Vázquez, and T. Gorin, *Phys. Rev. A* **95**, 022118 (2017).

- [32] A. Kenfack and K. Życzkowski, *J. Opt. B: Quantum Semiclass. Opt.* **6**, 396 (2004).
- [33] E. Cordero, M. de Gosson, M. Dörfler, and F. Nicola, *SIAM J. Math. Anal.* **50**, 2178 (2018).
- [34] M. de Gosson, *Symplectic Geometry and Quantum Mechanics* (Birkhäuser, Basel, 2006).
- [35] A. J. Dragt and S. Habib, How Wigner functions transform under symplectic maps, Quantum aspects of beam physics, in *Proceedings, Advanced ICFA Beam Dynamics Workshop, Monterey, USA, January 4-9, 1998*, edited by P. Chen (World Scientific, Singapore, 1998), pp. 651.
- [36] N. C. Dias, M. A. de Gosson, and J. N. Prata, *Proc. Amer. Math. Soc.* **142**, 3183 (2014).
- [37] E. Bonet-Luz and C. Tronci, *Proc. R. Soc. A: Math. Phys. Eng. Sci.* **472**, 20150777 (2016).
- [38] G. Manfredi and M. R. Feix, *Phys. Rev. E* **62**, 4665 (2000).
- [39] N. C. Dias, M. A. de Gosson, and J. N. Prata, *J. Fourier Anal. Appl.* **25**, 210 (2019).
- [40] R. Hanel and S. Thurner, *Europhys. Lett.* **96**, 50003 (2011).
- [41] M. Kalka, B. J. Spisak, D. Woźniak, M. Wołoszyn, and D. Kołaczek, *Sci. Rep.* **13**, 16266 (2023).
- [42] E. H. Hauge and J. A. Støvneng, *Rev. Mod. Phys.* **61**, 917 (1989).
- [43] M. Błaszak and Z. Domański, *Ann. Phys.* **327**, 167 (2012).
- [44] H. Weyl, *Z. Phys.* **46**, 1 (1927).
- [45] E. Wigner, *Phys. Rev.* **40**, 749 (1932).
- [46] M. E. Tuckerman, J. Alejandro, R. López-Rendón, A. Jochim, and G. J. Martyna, *J. Phys. A* **39**, 5629 (2006).
- [47] R. G. Littlejohn, *Phys. Rep.* **138**, 193 (1986).
- [48] F. J. Dyson, *Phys. Rev.* **75**, 486 (1949).
- [49] K. Mizuta and K. Fujii, *Quantum* **7**, 962 (2023).
- [50] M. Suzuki, *Proc. Jpn. Acad. Ser. B* **69**, 161 (1993).
- [51] G. Strang, *SIAM J. Numer. Anal.* **5**, 506 (1968).
- [52] D. Kołaczek, B. J. Spisak, and M. Wołoszyn, *Int. J. Appl. Math. Comp.* **29**, 439 (2019).
- [53] R. Cabrera, D. I. Bondar, K. Jacobs, and H. A. Rabitz, *Phys. Rev. A* **92**, 042122 (2015).
- [54] Z. Van Herstraeten and N. J. Cerf, *Phys. Rev. A* **104**, 042211 (2021).
- [55] N. C. Dias and J. N. Prata, *Ann. Henri Poincaré* **24**, 2341 (2023).
- [56] D. Chruściński and K. Młodawski, *Phys. Rev. A* **71**, 052104 (2005).
- [57] A. E. Bernardini and O. Bertolami, *J. Phys.: Conf. Ser.* **1275**, 012032 (2019).
- [58] S. H. Lie, S. Choi, and H. Jeong, *Phys. Rev. A* **103**, 042421 (2021).
- [59] A. Wobst, G.-L. Ingold, P. Hänggi, and D. Weinmann, *Eur. Phys. J. B* **27**, 11 (2002).
- [60] V. V. Dodonov, O. V. Man'ko, V. I. Man'ko, and A. Wünsche, *J. Mod. Opt.* **47**, 633 (2000).
- [61] D. Kołaczek, B. J. Spisak, and M. Wołoszyn, *Sci. Rep.* **11**, 11619 (2021).
- [62] A. M. Ozorio de Almeida, in *Entanglement and Decoherence: Foundations and Modern Trends*, edited by A. Buchleitner, C. Vivescas, and M. Tiersch (Springer, Berlin, 2008), pp. 157.
- [63] S. Kullback and R. A. Leibler, *Ann. Math. Statist.* **22**, 79 (1951).